THE JOURNAL OF COMPARATIVE NEUROLOGY 414:469–484 (1999)

Retinal Afferents to the Dorsal Raphe Nucleus in Rats and Mongolian Gerbils

KATHERINE V. FITE,[1]* SKIRMANTAS JANUŠONIS,[1] WARREN FOOTE,[2] AND LYNN BENGSTON[1]
[1]Neuroscience and Behavior Program, University of Massachusetts, Amherst, Massachusetts 01003
[2]Massachusetts General Hospital, Boston, Massachusetts 02114

ABSTRACT

A direct pathway from the retina to the dorsal raphe nucleus (DRN) has been demonstrated in both albino rats and Mongolian gerbils. Following intraocular injection of cholera toxin subunit B (CTB), a diffuse stream of CTB-positive, fine-caliber optic axons emerged from the optic tract at the level of the pretectum/anterior mesencephalon. In gerbils, CTB-positive axons descended ventromedially into the periaqueductal gray, moving caudally and arborizing extensively throughout the DRN. In rats, the retinal-DRN projection comprised fewer, but larger caliber, axons, which arborized in a relatively restricted region of the lateral and ventral DRN. Following injection of CTB into the lateral DRN, retrogradely labeled ganglion cells (GCs) were observed in whole-mount retinas of both species. In gerbils, CTB-positive GCs were distributed over the entire retina, and a nearest-neighbor analysis of CTB-positive GCs showed significant regularity (nonrandomness) in their distribution. The overall distribution of gerbil GC soma diameters ranged from 8 to 22 μm and was skewed slightly towards the larger soma diameters. Based on an adaptive mixtures model statistical analysis, two Gaussian distributions appeared to comprise the total GC distribution, with mean soma diameters of 13 (SEM ±1.7) μm, and 17 (SEM ±1.5) μm, respectively. In rats, many fewer CTB-positive GCs were labeled following CTB injections into the lateral DRN, and nearly all occurred in the inferior retina. The total distribution of rat GC soma diameters was similar to that in gerbils and also was skewed towards the larger soma diameters. Major differences observed in the extent and configuration of the retinal-DRN pathway may be related to the diurnal/crepuscular vs. nocturnal habits of these two species. J. Comp. Neurol. 414:469–484, 1999. © 1999 Wiley-Liss, Inc.

Indexing terms: subcortical vision; rodent visual system; environmental light stimulation; periaqueductal gray; retinal ganglion cells; serotonin

The serotonergic systems originating in the raphe nuclei of the brainstem have been implicated in a broad range of physiological, behavioral, and cognitive functions. Major functions of serotonin include the central regulation of autonomic functions, sensory and motor systems, cognition and associative learning, arousal and the sleep-wake cycle, as well as mood and emotional states (Jacobs and Fornal, 1993; Halliday et al., 1995; Cassel and Jeltsch, 1995; Montgomery, 1995; Dinan, 1996; Harvey, 1996; Simansky, 1996).

The dorsal raphe nucleus (DRN) of the mesencephalon contains the greatest proportion of serotonergic neurons, which represent 30–70% of all DRN neurons, depending on species (Wiklund et al., 1981; Stamp and Semba, 1995). These neurons give rise to ascending pathways that innervate widespread areas of the neocortex, striatum, and limbic system (Vertes, 1991). Each serotonergic neuron may influence a large number of postsynaptic neurons, and their postsynaptic effects are primarily modulatory and inhibitory at most target sites. The DRN also projects to a number of structures in the central visual system, including the superior colliculus (SC), lateral geniculate nucleus (LGN; Villar et al., 1988), intergeniculate leaflet (IGL; Meyer-Bernstein and Morin, 1996; Moga and Moore, 1997), and visual cortex (Koh et al., 1991). Activation of the DRN causes a pronounced inhibition of visual responses in

Grant sponsor: The WhiteHall Foundation; Grant sponsor: UMass-Baystate Collaborative Biomedical Research Program.

*Correspondence to: Dr. Katherine V. Fite, Neuroscience and Behavior Program, Tobin Hall, University of Massachusetts, Amherst, MA 01003. E-mail: kfite@psych.umass.edu

Received 5 February 1999; Revised 21 June 1999; Accepted 3 August 1999

most LGN neurons (Xue et al., 1996) and also may result in modulation of circadian phase (Rea et al., 1997) or block light-induced expression of the immediate early gene c-fos in the SCN (Meyer-Bernstein et al., 1997).

A direct pathway from the retina to the DRN has been reported in several mammalian species, including cats (Foote et al., 1978), rats (Shen and Semba, 1994; Kawano et al., 1996), and Mongolian gerbils (Fite et al., 1997). The existence of this pathway suggests that optic stimulation may directly influence DRN neurons. Previous reports also indicate that serotonin in the DRN exhibits a diurnal rhythm that is influenced by light-dark conditions and by the sleep-waking cycle (Cagampang et al., 1993; Cagampang and Inouye, 1994; Portas et al., 1998).

The present report describes and compares a number of neuroanatomical and morphological features associated with the retinal-DRN pathway in two species from the same family of rodents (Muridae): Mongolian gerbils, a crepuscular/diurnal species with a well-developed visual system (Susic and Masirevic, 1986; Mitrofanis and Finlay, 1990; Govardovskii et al., 1992), and the laboratory rat, a strongly nocturnal species. Preliminary results of the present study have been published in abstract form (Fite et al., 1997).

MATERIALS AND METHODS

Anterograde experiments

Intraocular injections of cholera toxin subunit B (CTB; low-salt; List Biological Laboratories, Campbell, CA) were used to identify retinal afferents in adult albino rats (*Rattus norvegicus*, Sprague Dawley, 300–800 g, n = 10) and in adult Mongolian gerbils (*Meriones unguiculatus*, 51–68 g, n = 20). All procedures used were approved by the Institutional Animal Care and Use Committee of the University of Massachusetts in accordance with NIH and USDA guidelines. Animals were anesthetized with an intraperitoneal injection (gerbils: ketamine [100 mg/kg] and xylazine [10 mg/kg]; rats: ketamine [90 mg/kg] and xylazine [4 mg/kg]). Following a topical application of corneal anesthetic (0.5% proparacaine hydrochloride), the needle of a 10 µl Hamilton microsyringe was inserted into the posterior chamber at the temporal cornea-conjunctival margin. Five microliters of 2% (w/v) solution of CTB in 2% dimethyl sulfoxide were slowly injected into the eye, and the needle was held in place for a period of 10–18 minutes. Following needle withdrawal, the injection site was immediately washed with saline and antibiotic (Bactracine) applied topically.

Following postinjection survival times of 4–10 days, animals were anesthetized and the exposed heart was injected with 1 ml (rats) or 0.2 ml (gerbils) of heparin (5,000 USP units/ml). Animals were then perfused transcardially with saline followed by 400 ml (rats with the descending aorta clamped) or 300 ml (gerbils) of chilled 4% paraformaldehyde in 0.1 M phosphate buffer (PB; pH 7.2). The brain was subsequently removed, postfixed in the same fixative overnight at 4°C and then transferred to 30% sucrose in PB overnight. Coronal 40-µm-thick sections were cut on a freezing microtome; sections were saved from midthalamic to caudal midbrain levels.

Brain sections were processed using a highly sensitive immunocytochemical protocol (Angelucci et al., 1996). Sections were rinsed in 0.1 M phosphate-buffered saline (PBS; pH 7.4), incubated in 0.3% H_2O_2 in PBS for 20 minutes, rinsed in PBS (three times, 5 minutes each), and incubated in 0.1 M glycine in PBS for 30 minutes. Following three rinses (5 minutes each) in PBS, sections were incubated in 4.5% normal rabbit serum (NRS; Vector, Burlingame, CA), 2.5% bovine serum albumin (BSA; Sigma, St. Louis, MO), and 0.4% Triton X-100 (Tx) in PBS overnight at 4°C. Sections were rinsed two times (5 minutes each) in PBS and incubated in a goat anti-CTB antibody (List Biological Laboratories) solution (antibody dilution 1:4,000–1:2,700) in PBS, containing 2% NRS, 2.5% BSA, 2% Tx for 4 days at 4°C. Sections were rinsed four times (15 minutes each) in PBS; incubated in 2% NRS and 2.5% BSA in PBS for 10 min; then incubated in biotinylated rabbit anti-goat IgG antibody (Vector; diluted 1:200) with 2% NRS, 2.5% BSA, and 1% Tx in PBS for 1.5 hours. [In some animals, the biotinylated rabbit anti-goat antibody was replaced by biotinylated donkey anti-goat IgG antibody (Jackson Immunoresearch Laboratories; 1:1,000) and the rabbit serum with donkey serum (Jackson Immunoresearch Laboratories). This yielded very low background staining]. Sections were rinsed four times (15 minutes each) in PBS and incubated again in 2% NRS and 2.5% BSA in PBS for 10 minutes. Sections were incubated in a 1:100 ABC (ABC Elite; Vector) solution in PBS for 1 hour, rinsed four times in PBS (15 minutes each), then rinsed twice (5 minutes each) in 0.05 Tris buffer (TB; pH 7.4), incubated in 0.5–1% $CoCl_2$ in TB for 10 minutes, then rinsed in TB for 1 minute, followed by two rinses in PBS (5 minutes each). Sections were then preincubated in diaminobenzidine (DAB; 0.05%) in PBS for 5 minutes and reacted for 3 minutes by adding 0.01% H_2O_2 to the DAB solution. Sections were then rinsed five times (1 minute each) in PBS, mounted on chromium-subbed slides, allowed to air dry, cleared with xylenes or Hemo-De, and coverslipped with Permount. Sections containing CTB-labeled axons and terminal profiles were charted with reference to a standard rat atlas (Paxinos and Watson, 1998) using both bright- and darkfield microscopy. At least three cases showing the highest levels of CTB immunoreactivity in central visual nuclei were analyzed for each species.

Retrograde experiments

Pressure injections of CTB were placed in the DRN of rats and gerbils as follows. The animal was placed in a Kopf, small-animal stereotaxic apparatus and the incisor bar adjusted so that the dorsal surface of the skull was level. By using a dental drill, a small burr hole was made in the skull, posterior to lambda (3.5 mm in gerbils and 4.9 mm in rats). A 10 µl Hamilton syringe was inclined posteriorly at a 35° angle from vertical and was positioned with the needle tip just touching the surface of the dura. The needle was then advanced slowly for 6.1 mm in gerbils or 8.5 mm in rats. CTB (0.5–0.8 µl) was gradually injected over a 5 minute period. The needle was left in place for at least 10 minutes following completion of the injection and was then slowly withdrawn. The skull was sealed with bone wax and the skin incision closed with wound clips. Following a survival time of 7 days, animals were perfused transcardially with 4% paraformaldehyde. The brain was removed, postfixed for 4–6 hours, and placed in 30% sucrose in PB overnight. The next day, 40-µm-thick coronal sections were cut on a freezing microtome; serial sections were saved from midthalamic to caudal midbrain levels.

Following perfusion, each eye was removed, injected with a small quantity of fixative, and immersed in fixative for 1 hour. The retina was removed intact, and the retinal pigment epithelium was gently brushed away from the posterior surface. The retina was then cut into four quadrants along the vertical and horizontal meridians. Individual quadrants were placed in small vials and postfixed at 4°C in 4% paraformaldehyde, overnight, prior to immunocytochemical processing the following day.

Immunocytochemistry

Immunocytochemistry was performed on brain sections on the same day they were cut, together with retinal quadrants from both eyes of the same animal (method of Mikkelsen, 1992). Tissues were rinsed three times (10 minutes each) in 0.1 M PBS (pH 7.4), incubated in 1% H_2O_2 in PBS for 10 minutes, rinsed three times (5 minutes each) in PBS, incubated in 4% NRS with 0.3% Tx and 0.5% BSA in PBS for 20 minutes, and then incubated in goat anti-CTB antibody (diluted 1:4,000) in PBS containing 0.3% Tx and 1% BSA for 3 days at 4°C. Following incubation, tissues were rinsed three times (10 minutes each) in PBS containing 0.1% Tx (PBS-Tx) and were then incubated for 60 minutes in biotinylated rabbit anti-goat IgG antibody (1:600) in PBS-Tx containing 0.25% BSA, rinsed three times (10 minutes each) in PBS-Tx, incubated for 60 minutes in streptavidin-HRP (1:1,000, Jackson Immunoresearch) in PBS-Tx containing 0.25% BSA, and rinsed two times (10 minutes each) in PBS-Tx and once (10 minutes) in 0.05M Tris-buffer (TB, pH 7.6). After a 1 minute soak in 0.05% DAB in TB, 0.01% H_2O_2 was added, and retinal quadrants and brain sections were reacted for 5 min. Tissues were then rinsed two times (5 minutes each) in TB and two times (5 minutes each) in PBS. Retinal quadrants were transferred from PBS to distilled water and immediately mounted onto subbed slides, ganglion cell layer upward, with each retinal quadrant restored to its original location relative to the center of the eye. Retinal flat mounts were allowed to dry on the slide for approximately 1 hour, then cleared with a quick dip into Hemo-De and coverslipped with a thick layer of Permount.

A set of reference sections also was prepared for each species in which the location of serotonergic neurons was demonstrated, immunocytochemically, using antibodies against serotonin (5-HT) in order to define the boundaries of the DRN. Animals were perfused as described above, brains were postfixed overnight at 4°C, then immersed in 30% sucrose in PB overnight, and serial sections were cut on a freezing microtome at 40-μm-thickness throughout the mesencephalon. For 5-HT immunocytochemistry, the CTB protocol (Angelucci et al., 1996) described above was used, with the following modifications. The goat anti-CTB antibody was replaced with rabbit anti-5-HT antibody (Protos Biotech, New York, NY; NT102) at a dilution of 1:1,500, the rabbit anti-goat antibody was replaced with goat anti-rabbit IgG antibody (Vector) diluted 1:200, and the rabbit serum was replaced with goat serum.

Analysis of retinal ganglion cells

CTB-positive ganglion cell profiles were identified in both retinas of three gerbils and three rats with well-placed CTB injections into the lateral DRN. CTB-positive ganglion cell (GC) profiles were identified using an oil-immersion objective (×100) and were traced using a camera lucida. Further quantification and analysis were accomplished using a computer-assisted morphometry system (Jandel Scientific) and statistical software package (Systat). Both the intercellular spacing and the density of CTB-labeled GCs were obtained in ten sample areas from the gerbil retina that contained the greatest number of retrogradely labeled GCs. Five sample areas were randomly selected both from the superior retina and from the inferior retina (ten areas total). Sample areas were circular and ranged from 0.7 to 1.1 mm^2 (mean 0.96 mm^2). By using a camera lucida, the location of individual CTB-positive ganglion cells was charted in each sample area. The total area sampled was 9.67 mm^2, which represented approximately 20% of the total retina (50 mm^2).

An estimate of the total number of ganglion cells projecting to the DRN was obtained from this same retina. For each of ten sample areas, the cellular density of labeled cells per square millimeter was obtained, and a mean density of CTB-positive GCs/mm^2 was then estimated for the entire retina. Similar procedures were used in the rat retina containing the greatest number of retrogradely labeled GCs following CTB injection into the DRN. However, in rats, nearly all CTB-positive GCs occurred in the inferior retina, thereby limiting soma size measures to this portion of the retina.

To assess the degree of regularity associated with the spatial distribution of DRN-projecting GCs, the nearest-neighbor distance (NND) from each CTB-positive GC to its nearest neighbor was measured in ten sample areas (n = 259), and these values were plotted as a frequency distribution. The most commonly used estimator of mosaic regularity, the "conformity ratio" (CR; the ratio of the mean NND to the standard deviation of the distribution of intercellular distances) was calculated as described by Cook (1996). Using Cook's ready-reckoner values (previously obtained from a set of empirically determined critical values of the CR) for a sample size of 259, the statistical probability of regularity was determined for the DRN-projecting GC population. In addition, the total distribution of DRN-projecting GC soma diameters was analyzed, statistically, using the adaptive mixtures algorithm, a semiparametric method that assesses the probability-density function of a given distribution as a mixture of Gaussian (normal) densities (see Advanced Computation Technology Group, Department of Defense; www.nswc.navy.mil/compstat/AM).

RESULTS

Anterograde observations: Retinal afferents

Retinal terminals in all primary thalamic and mesencephalic central visual nuclei were strongly immunoreactive for CTB 5–7 days following intraocular injections. In addition, several hypothalamic nuclei and periventricular cellular regions contained CTB-immunoreactive retinofugal axons, as previously reported for other species by investigators using CTB as an anterograde tracer for retinal afferents (see Ling et al., 1998; Youngstrom et al., 1991). In the present report, primary emphasis was placed on analysis of retinofugal afferents to the mesencephalic periaqueductal gray (PAG) and to the DRN.

In gerbils, CTB-positive retinal axons emerged from the contralateral optic tract at several locations. At the level of the pretectum and rostral superior colliculus (SC), a stream of CTB-positive axons descended from the optic tract (Figs. 1, 2). These axons were of fine caliber and descended along an oblique trajectory, through the inter-

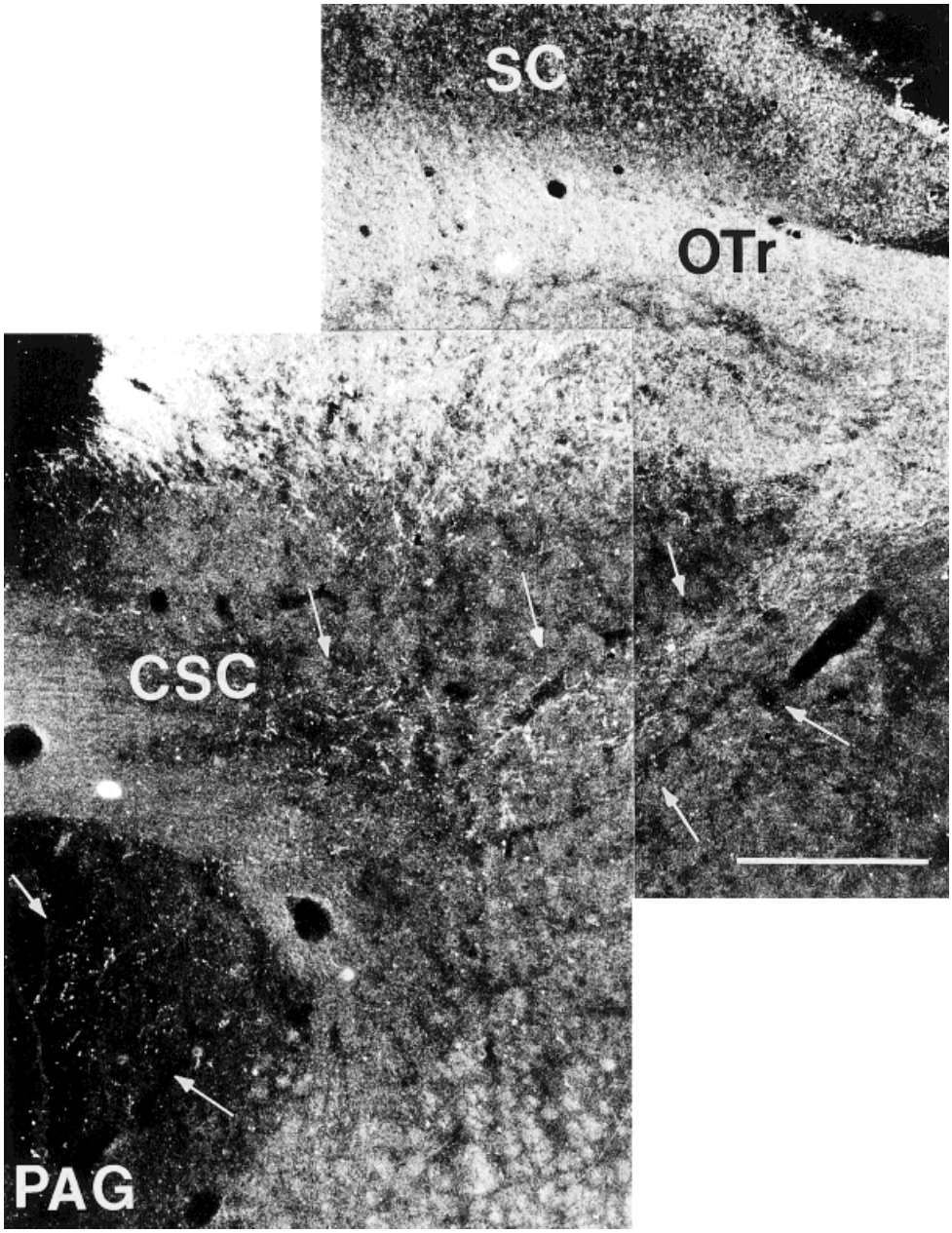

Fig. 1. Darkfield photomontage of CTB-positive optic axons emerging from the gerbil optic tract (OTr) at the level of the rostral superior colliculus (SC) and coursing medially, through the comissure of the superior colliculus (CSC), into the periaqueductal gray (PAG). Arrows indicate the approximate boundaries of this axonal stream. Scale bar = 200 μm.

nal and deep gray layers of the SC, passed through the commissure of the superior colliculus, and entered the PAG (Fig. 3). More caudally, several diffuse streams of CTB-positive retinal axons also descended into the PAG. Some of these axons showed en passant varicosities and short branches as they descended through the PAG, along the cerebral aqueduct (Fig. 4). More caudally, a small number of CTB-positive axons descended into the lateral margins of the PAG and coursed ventrally to enter the lateral margins and main body of the DRN, where they formed a dense matrix of extremely fine, terminal-like arborizations with numerous varicosities (Figs. 5, 6).

The extent of the retinal terminal field in the DRN was extensive in gerbils, and all but the most caudal and ventrolateral regions of the DRN contained CTB-positive axonal arborizations. CTB-positive, varicose, retinal afferents were observed rostrocaudally from the level of the oculomotor nucleus (nIII) to the level of the dorsal tegmental nucleus (rostrocaudal distance approximately 1,300 μm; Fig. 7). Mediolaterally, optic afferents extended from the lateral margins of the DRN, across the main body of the DRN, including the area immediately ventral to the aqueduct (Fig. 5). In gerbils, optic-axonal varicosities ranged in size from 0.6 to 2.4 μm. The distribution of

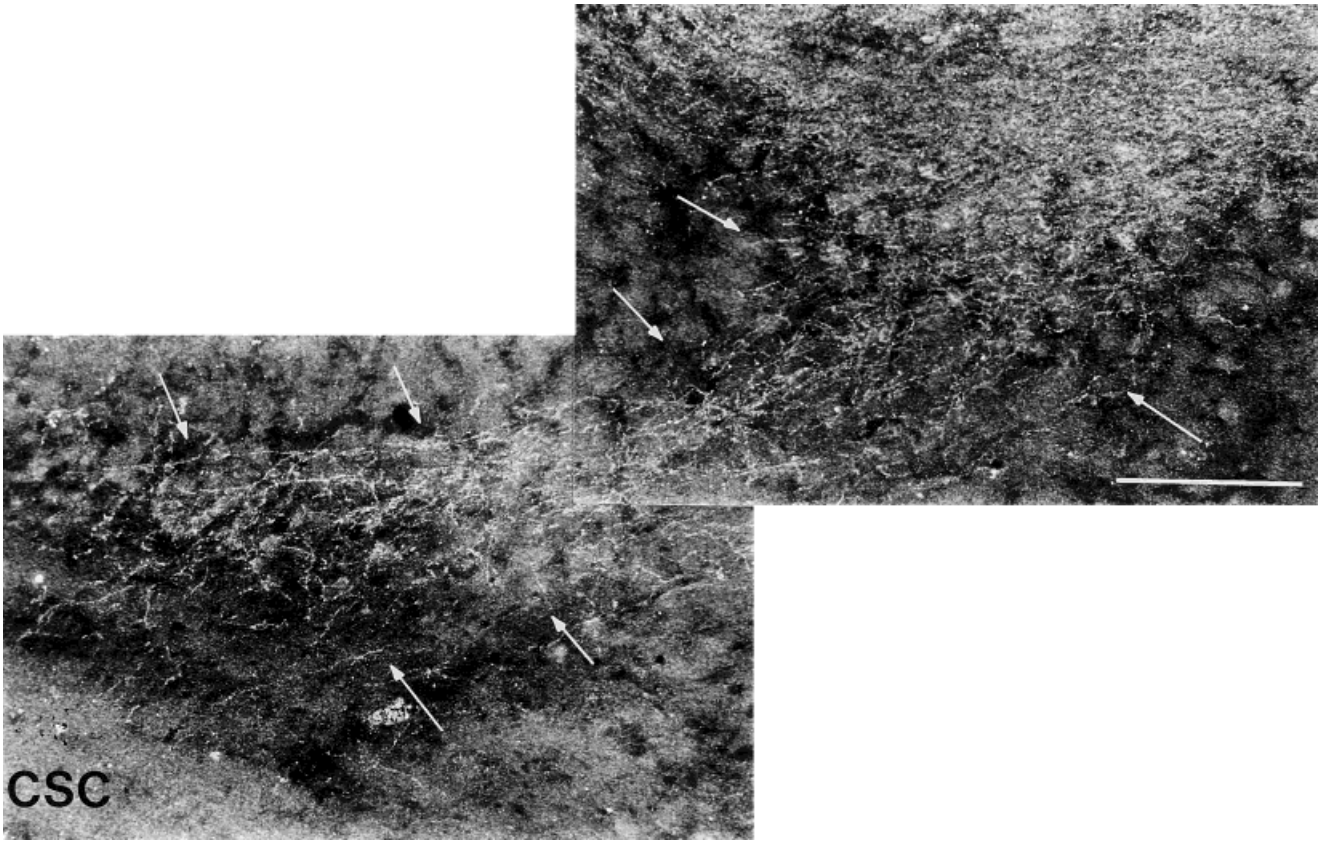

Fig. 2. Darkfield photograph of CTB-positive gerbil optic axons (arrows) descending from the optic tract towards the commissure of the superior colliculus (CSC). Scale bar = 100 μm.

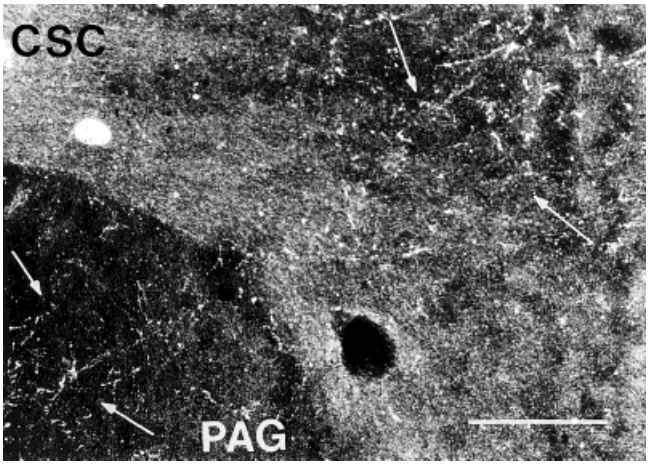

Fig. 3. Darkfield photograph of CTB-positive gerbil axons (arrows) passing through the commissure of the superior colliculus (CSC) and entering the periaqueductal gray (PAG). Scale bar = 100 μm.

CTB-positive, afferent arborizations was bilaterally symmetrical, regardless of whether intraocular injections were monocular or binocular. All optic afferents appeared to originate from the contralateral optic tract. Small numbers of CTB-positive retinal afferents also were observed entering the nucleus cuneiformis, which lies immediately adjacent to the DRN at its most caudal and lateral margins.

In rats, CTB-positive axons descended from the optic tract at the level of the pretectum and followed a trajectory similar to that observed in gerbils (Fig. 8A); likewise, these axons entered the PAG and descended ventrally along the edge of the aqueduct (Fig. 8B). However, in the rat, CTB-positive axons did not form the extensive, rostrocaudal, DRN terminal plexus that was observed in gerbils; instead, a smaller region of CTB-positive axonal arborizations was observed in the DRN lateral wings (Fig. 9). The caliber of both axons and their varicosities was larger in rats (0.8–4.0 μm) than in gerbils (0.6–2.4 μm). Retinal afferents were also seen bilaterally in rats, but the density of axonal arborizations was consistently greater in the contralateral DRN of rats.

Retrograde observations: Retinal ganglion cells

In three gerbils with well-placed, unilateral CTB injections of the lateral DRN (Fig. 10), CTB immunoreactivity was limited to the injection site and its immediate vicinity, with no leakage of the tracer into the SC, pretectum, or other retinorecipient nuclei. The combined distribution of CTB-positive, GC soma diameters from both retinas of three gerbils with unilateral DRN injections ranged from 8 to 22 μm (n = 1,330, mean = 14 μm; SEM ±0.65 μm). No differences were found in ipsilateral vs. contralateral GC soma sizes. The combined GC distribution was somewhat

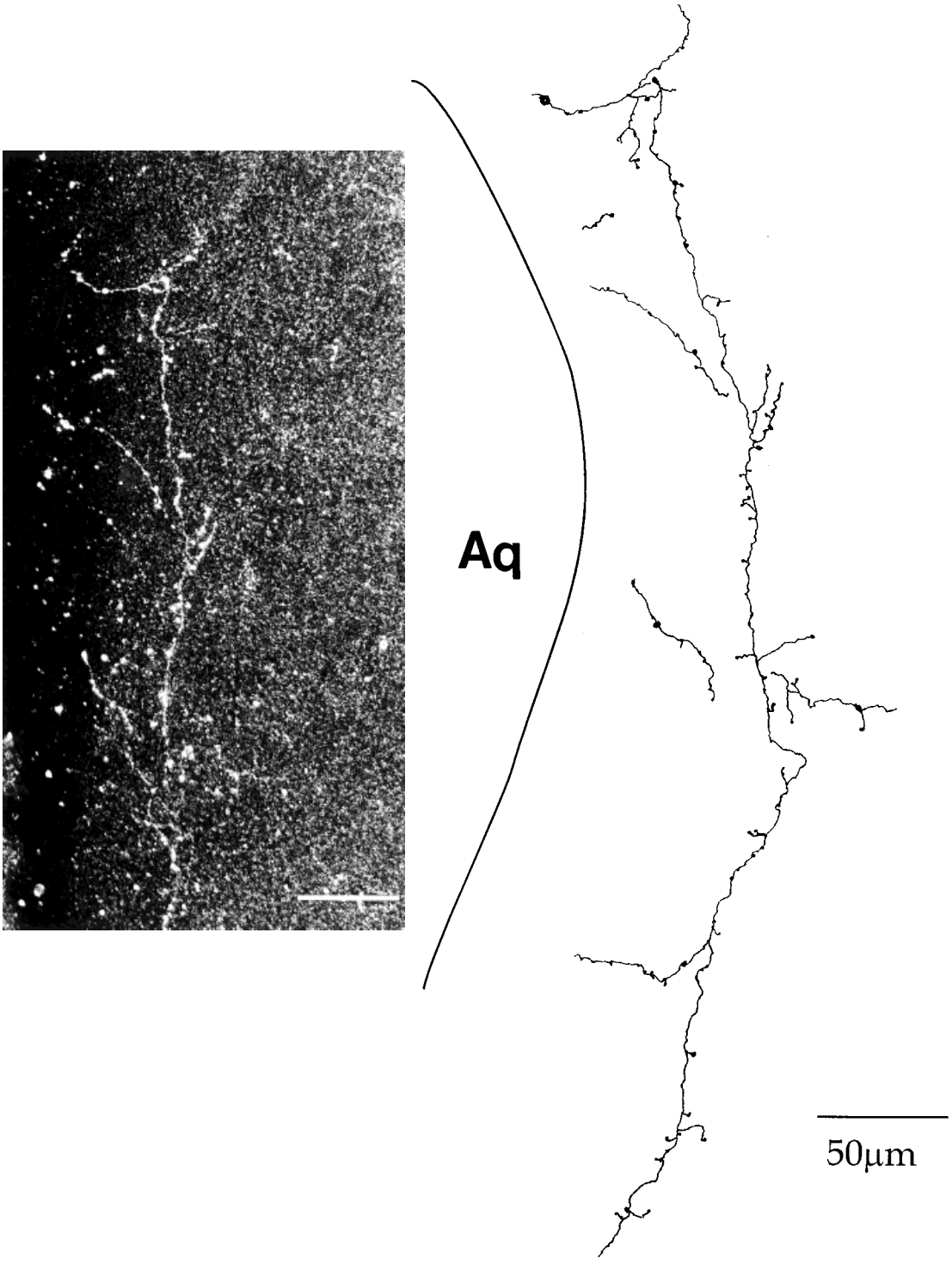

Fig. 4. Darkfield photograph and camera lucida tracing of the same CTB-positive optic axon in the gerbil periaqueductal gray adjacent to the cerebral aqueduct (Aq). Scale bars = 50 μm.

skewed towards the larger soma diameters (Fig. 11), and the adaptive mixtures model analysis indicated that the observed population of gerbil GC soma diameters consisted of two Gaussian distributions. The larger subpopulation contained 83% of the total (mean = 13 μm; SEM ±1.7 μm); the smaller subpopulation contained the

Fig. 5. **A:** Serotonin-immunoreactive neurons in the gerbil dorsal raphe nucleus (DRN) used to define the boundaries of the DRN. **B:** CTB-positive optic axonal arborizations in the gerbil dorsal raphe nucleus shown in darkfield illumination. **C:** CTB-positive optic axonal arborizations in the dorsomedial portion of the gerbil dorsal raphe nucleus. Aq, cerebral aqueduct. Scale bars = 200 μm in A,B; 100 μm in C.

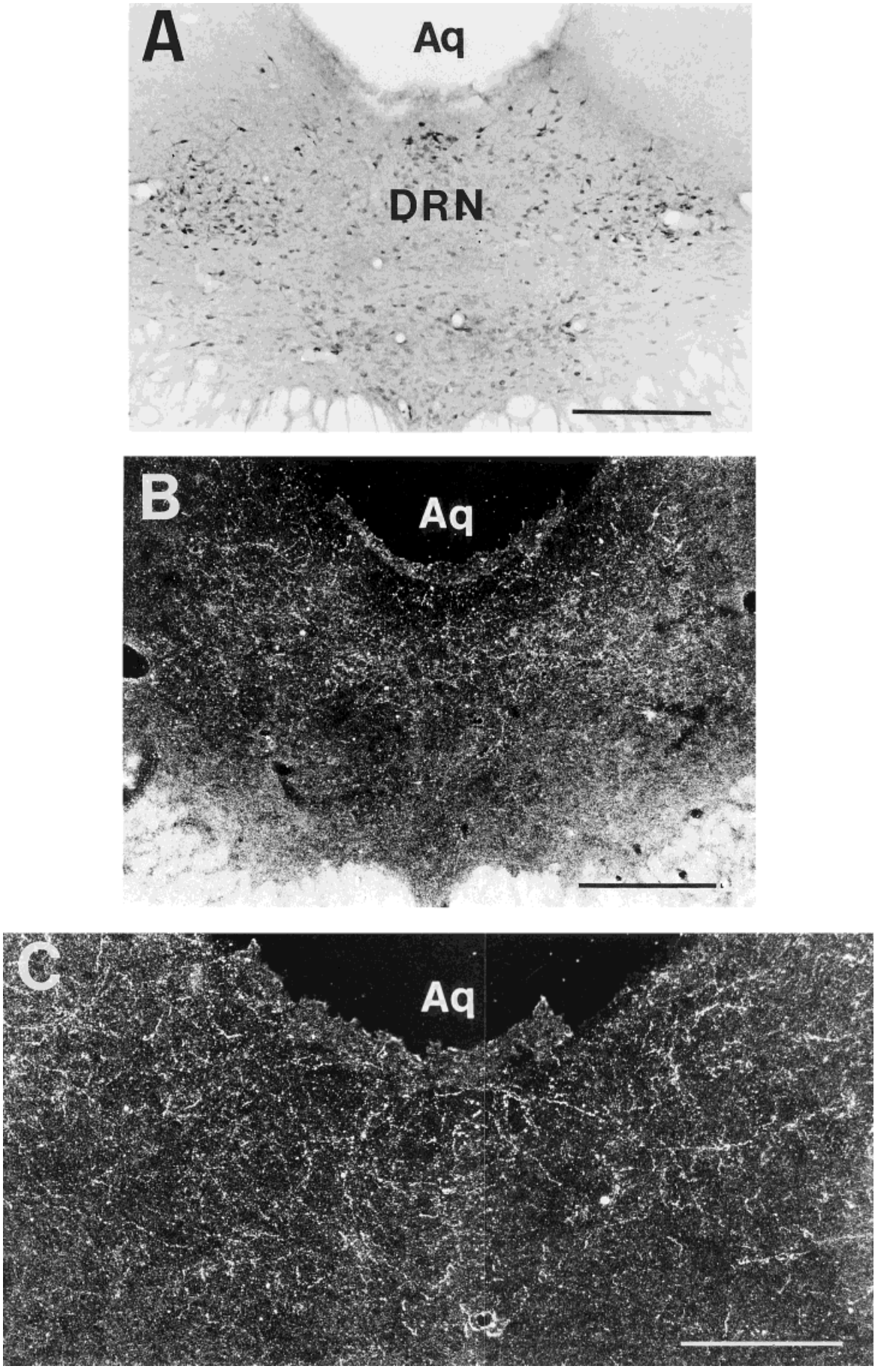

Figure 5

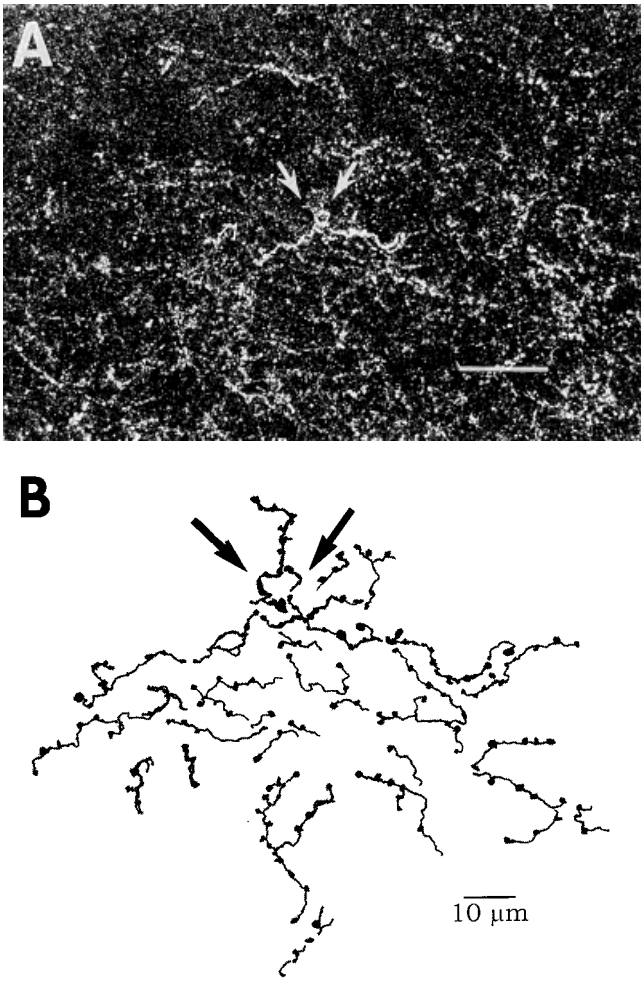

Fig. 6. **A:** CTB-positive optic axonal arborizations (darkfield photograph) in the gerbil dorsal raphe nucleus. For reference in B, arrows indicate a loop-like configuration. **B:** Higher magnification camera lucida tracing of axonal arborizations and varicosities from a region indicated by arrows in A. Scale bars = 50 μm in A; 10 μm in B.

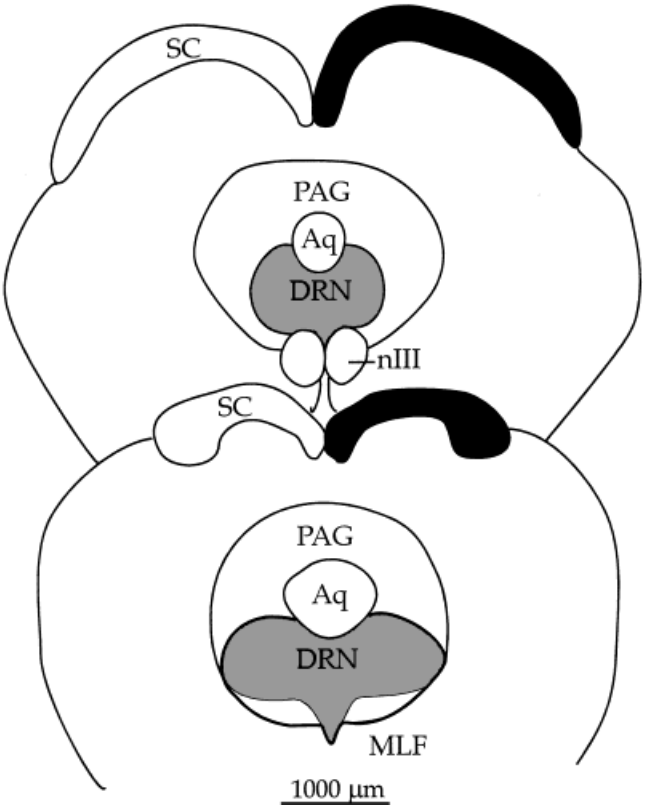

Fig. 7. Schematic representation of two coronal sections showing the location and extent of CTB-positive optic axonal arborizations (light shading) in the rostral (top) and caudal (bottom) dorsal raphe nucleus (DRN) in gerbils. Heavy line indicates the full extent of the DRN. Dark shading indicates CTB-positive terminals in the superior colliculus (SC) contralateral to the injected eye. Aq, cerebral aqueduct; mlf, medial longitudinal fasciculus; PAG, periaqueductal gray; nIII, oculomotor nucleus. Scale bar = 1,000 μm.

remaining 17% of the distribution (mean = 17 μm; SEM ± 1.5 μm).

A combined population of 875 well-labeled GCs were analyzed from both eyes of one gerbil (G70, left, ipsilateral eye 430; right, contralateral eye 445). In many CTB-positive GCs, one to three primary dendrites were labeled, and conspicuous dendritic varicosities, occurring at regular intervals, were visible (Fig. 12). CTB-positive GCs appeared to be regularly distributed, indicating a nonrandom, mosaic coverage of the entire retina by DRN-projecting GCs (Fig. 13). In the most well-labeled case (G70, right retina), the mean nearest-neighbor distance between adjacent CTB-labeled ganglion cells was 107 ± 4 μm. The ratio of the mean to the SD (49.8 μm) yielded a conformity ratio (CR) of 2.14. For a sample size of 259, this CR value implies significant ($P < 0.01$) nonrandomness (e.g., regularity) in the distribution of these DRN-projecting GCs (see Cook, 1996). Based on a cellular-density analysis, the number of CTB-positive ganglion cells in this gerbil retina was estimated to be 1,674.

By comparison, many fewer CTB-positive GCs were observed in rats following unilateral injections of CTB into the DRN. In the rat, CTB-positive GCs occurred almost exclusively in the inferior retina of both eyes. Rat GC soma diameters ranged from 10 to 21 μm (mean = 14 μm). The distribution of CTB-positive, GC soma diameters for three rats (n = 244) and three gerbils (n = 1330) is shown in Figure 11. As was observed in gerbils, regularly spaced varicosities often were seen on the dendrites of many of the larger CTB-positive rat GCs (Fig. 14). Because of the variable density of CTB labeling in rat GC somas, no estimates could be made of the total number of CTB-positive ganglion cells or their intercellular spacing.

DISCUSSION

Retinal-DRN projection

The present study has demonstrated the existence of a direct, retinal-DRN projection in both rats and gerbils, although several species differences were observed. In gerbils, the descending pathway was larger and more conspicuous, and both the density of terminals and the extent of the terminal field were greater and more well-defined in gerbils than in rats. In general, the course of retinal afferents to the DRN appeared to be similar in both species, axons emerging from the optic tract at the level of the pretectum/anterior superior colliculus, coursing ventro-

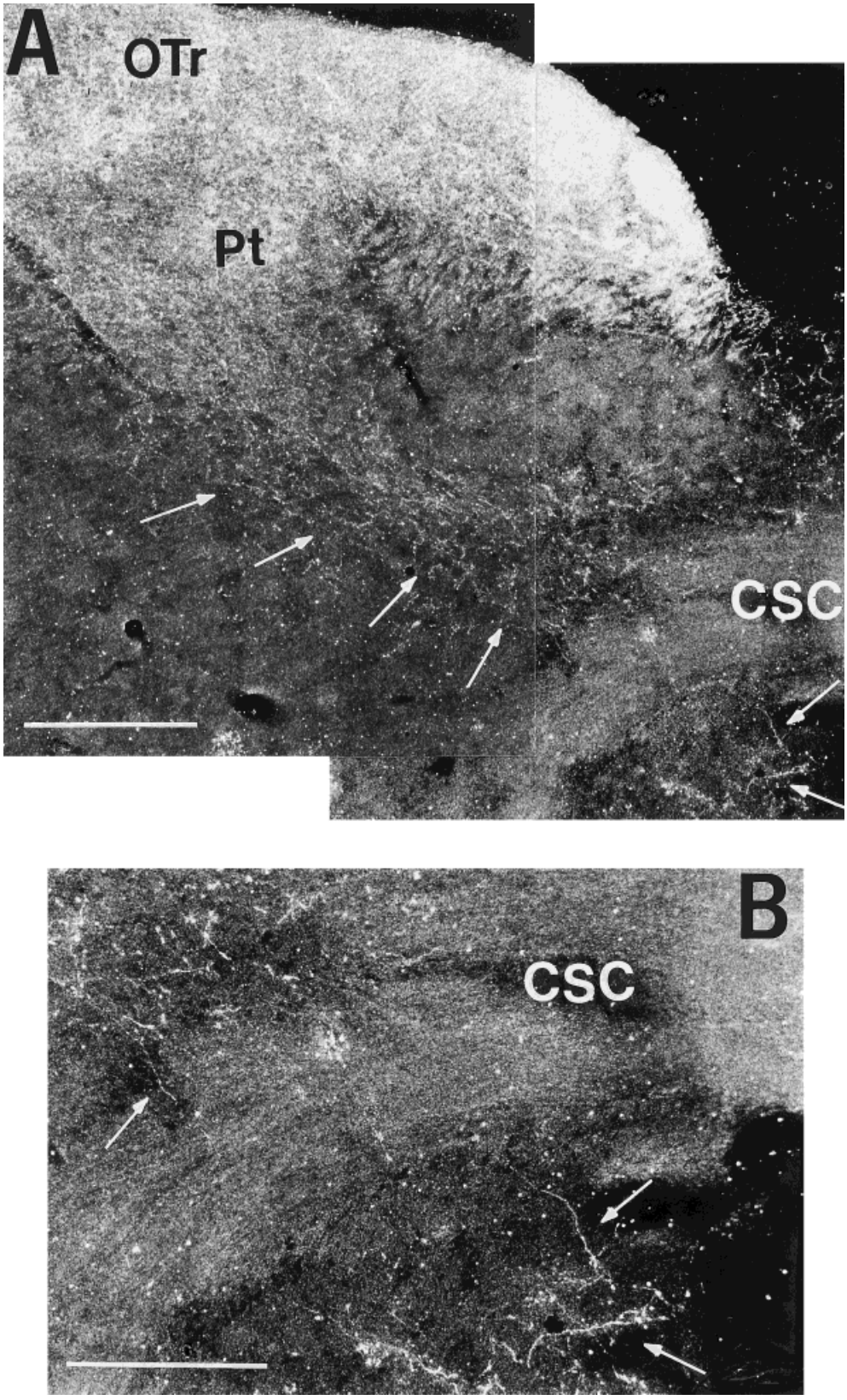

Fig. 8. **A:** Darkfield photomontage of CTB-positive rat optic axons (arrows) descending from the optic tract (OTr) at the level of the pretectal region (Pt), moving medially through the commissure of the superior colliculus (CSC) into the periaqueductal gray. **B:** Higher magnification from A, in the region of the CSC, showing optic axons (arrows) entering the periaqueductal gray. Scale bars = 200 μm in A; 100 μm in B.

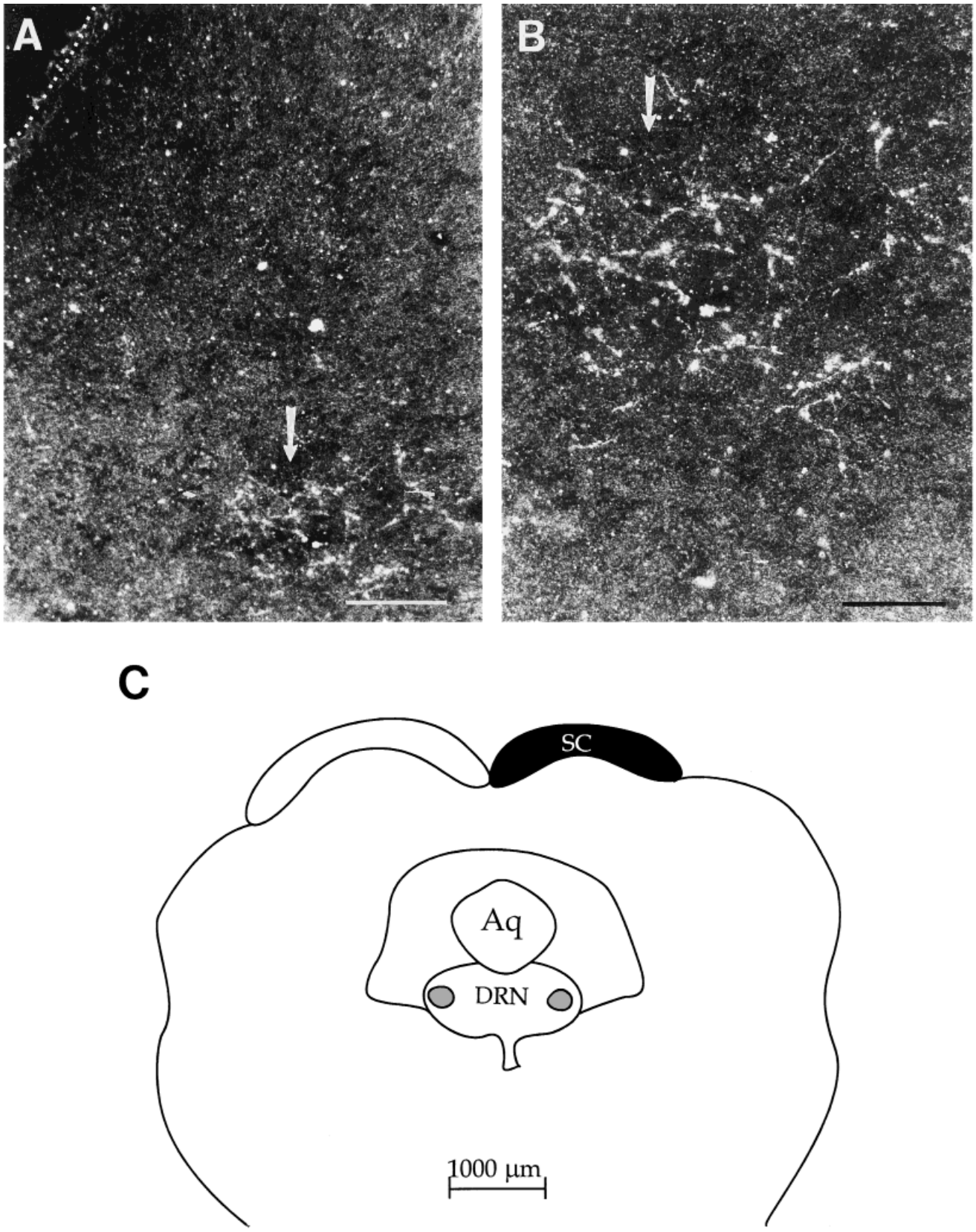

Fig. 9. **A:** CTB-positive optic axonal arborizations (arrow) in the rat dorsal raphe nucleus (DRN). Dotted line (upper left) indicates boundary of the cerebral aqueduct. Arrow indicates region shown at higher magnification in B. **B:** Enlarged view of CTB-positive axons in the lateral DRN as shown in A. **C:** Schematic representation of a coronal section from the caudal pole of the rat DRN. Small, shaded areas indicate location of CTB-positive, optic axonal arborizations. Scale bars = 200 μm in A; 50 μm in B; 1,000 μm in C.

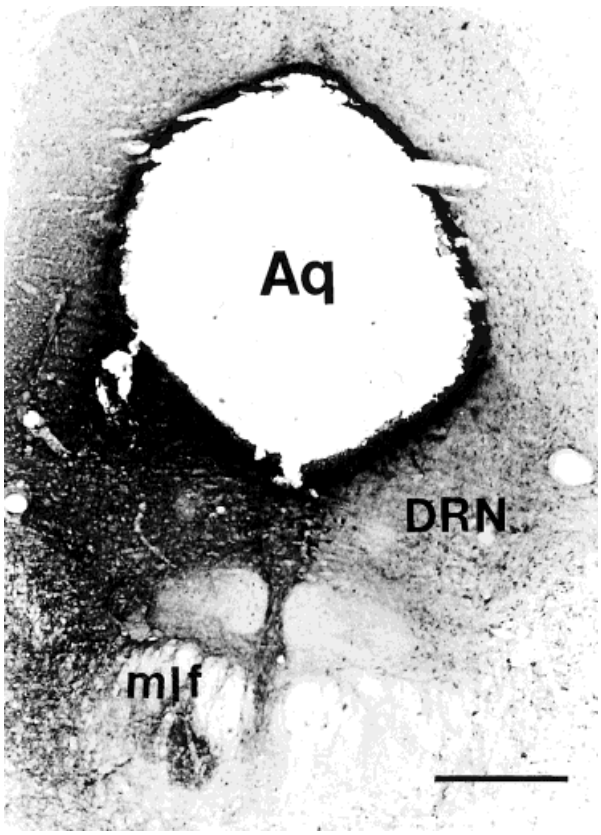

Fig. 10. Representative CTB injection site in the lateral portion of the gerbil dorsal raphe nucleus (DRN); breaks in the tissue around the cerebral aqueduct (Aq) are tissue artifacts incurred during frozen sectioning. mlf, medial longitudinal fasciculus. Scale bar = 500 μm.

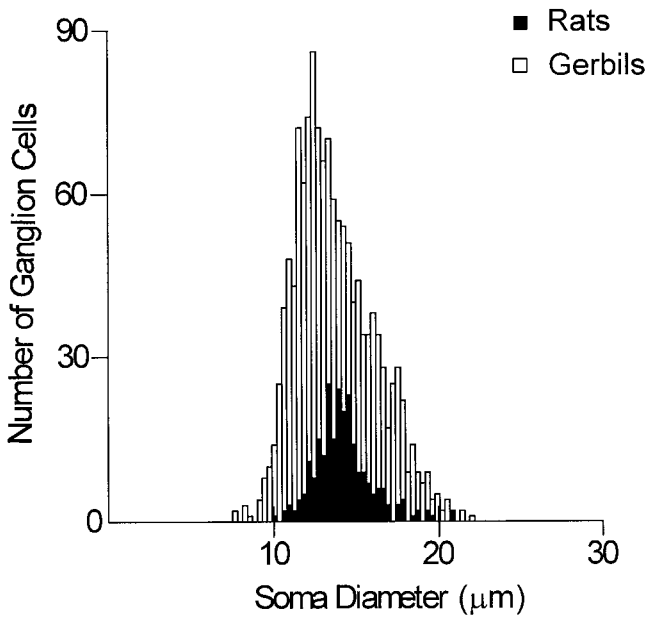

Fig. 11. Combined frequency distribution of retrogradely labeled ganglion cell soma diameters of three gerbils (light bars; n = 1330) and three rats (dark bars; n = 244) after injections of CTB into the lateral DRN.

medially through the commissure of the superior colliculus, and descending into the PAG, as previously described for rats (Shen and Semba, 1994). The calibers of descending axons and their en passant varicosities were larger and ramified in a more restricted region of the ventrolateral DRN in rats than in gerbils, where retinal afferents were observed over the entire rostrocaudal extent of the lateral and dorsomedial portions of the DRN.

In both species, CTB injections into the lateral DRN retrogradely labeled GCs with a similar range of soma diameters. However, following DRN injections, approximately four to five times as many CTB-positive GCs were retrogradely labeled in gerbils as in rats, consistent with the more extensive retinal-DRN pathway and terminal zone observed in gerbils. The distribution of gerbil GC soma diameters was slightly skewed towards the larger soma diameters, suggesting that more than one population of GCs contributed to this retinofugal projection. This hypothesis was confirmed using a mixed-model statistical analysis, which revealed two Gaussian components in the overall distribution. The larger subpopulation of DRN-projecting GCs in gerbils had a smaller mean soma diameter (13 μm, SEM ±1.7 μm) than did the second subpopulation (17 μm, SEM ±1.5 μm). Retrograde labeling of GCs via the transected optic nerve with the carbocyanine dye 1,1dioctadecyl-3–3,-3′,-3′-tetramethylindocarbocyanine percholate (DiI) has shown that the total population of gerbil GC soma diameters ranges from 6 to 26 μm (McLaughlin and Fite, unpublished results). Previous studies in the rat retina have shown that GC soma diameters range from 6 to 35 μm (Moore et al., 1995; Leak and Moore, 1997; Huxlin and Goodchild, 1997). In the present study, a range of 10–21 μm was obtained for DRN-projecting GC soma diameters in rats. Therefore, in both rats and gerbils, neither the smallest nor the largest GCs appear to contribute to the retinal-DRN projection. Possibly, some or all retinal axons to the DRN are collaterals of axons projecting to other retinorecipient nuclei, such as the SC and/or pretectal optic nuclei, given the locations at which retinal-DRN axons emerge from the optic tract. Additional studies utilizing double-labeling techniques will be necessary to resolve this question.

Retinal ganglion cells projecting to the DRN

With regard to their retinal distribution, in gerbils GCs projecting to the DRN appeared to be regularly spaced, suggesting a mosaic-like coverage of the entire retina. Cellular mosaics have been described in all layers of the retina (Cook, 1996) and have been useful as one criterion in identifying independent neuronal classes (Cook, 1998). In rats, nearly all retrogradely labeled GCs were observed in the inferior retina. Following injection of retrograde tracers into the rat DRN, Shen and Semba (1994) also described a small population of GCs confined to one-half of the retina. The species differences observed in the present study could be due, in part, to differences in the location of DRN injection sites and/or the area of effective CTB uptake by DRN retinal afferents. In rats, the region containing retinal axonal arborizations was considerably smaller and more localized than in gerbils and would be less likely to be located at or near the center of an injection site. By comparison, in gerbils, optic afferents arborized extensively throughout the lateral and dorsomedial DRN; therefore, the specific placement of the injection site would

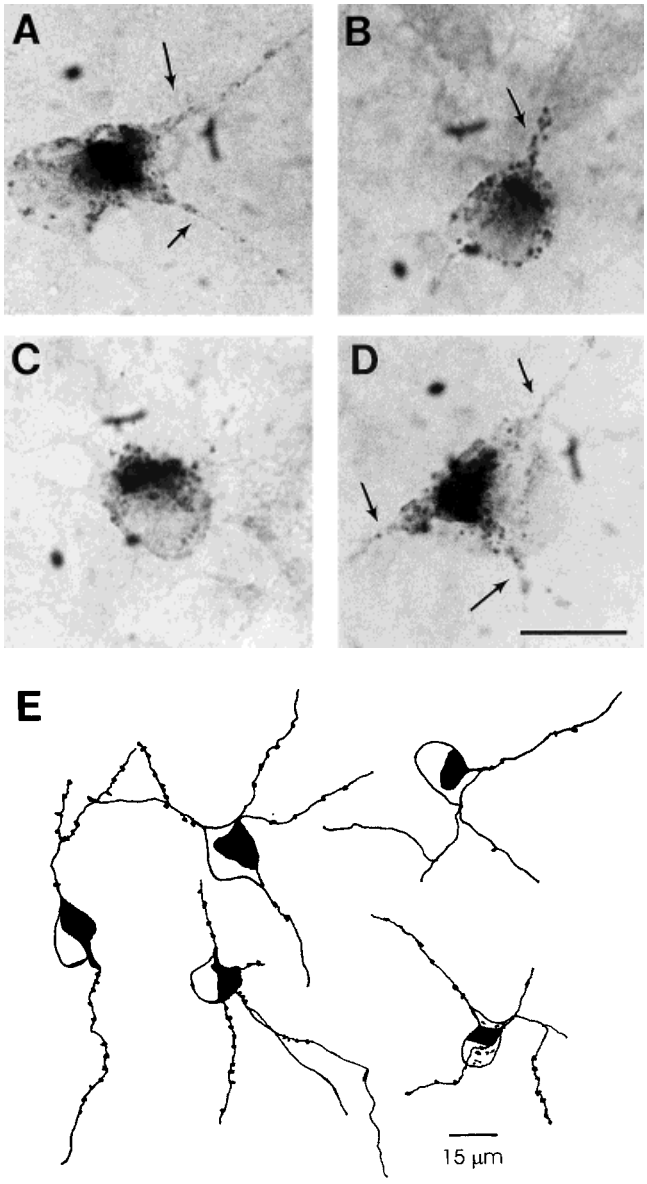

Fig. 12. **A–D:** CTB-positive gerbil ganglion cells photographed in whole-mount retinas following CTB injection into the lateral dorsal raphe nucleus. Arrows indicate primary dendrites labeled with CTB. **E:** Camera lucida tracings of CTB-positive gerbil ganglion cells (intercellular spacing is arbitrary). Scale bars = 15 μm.

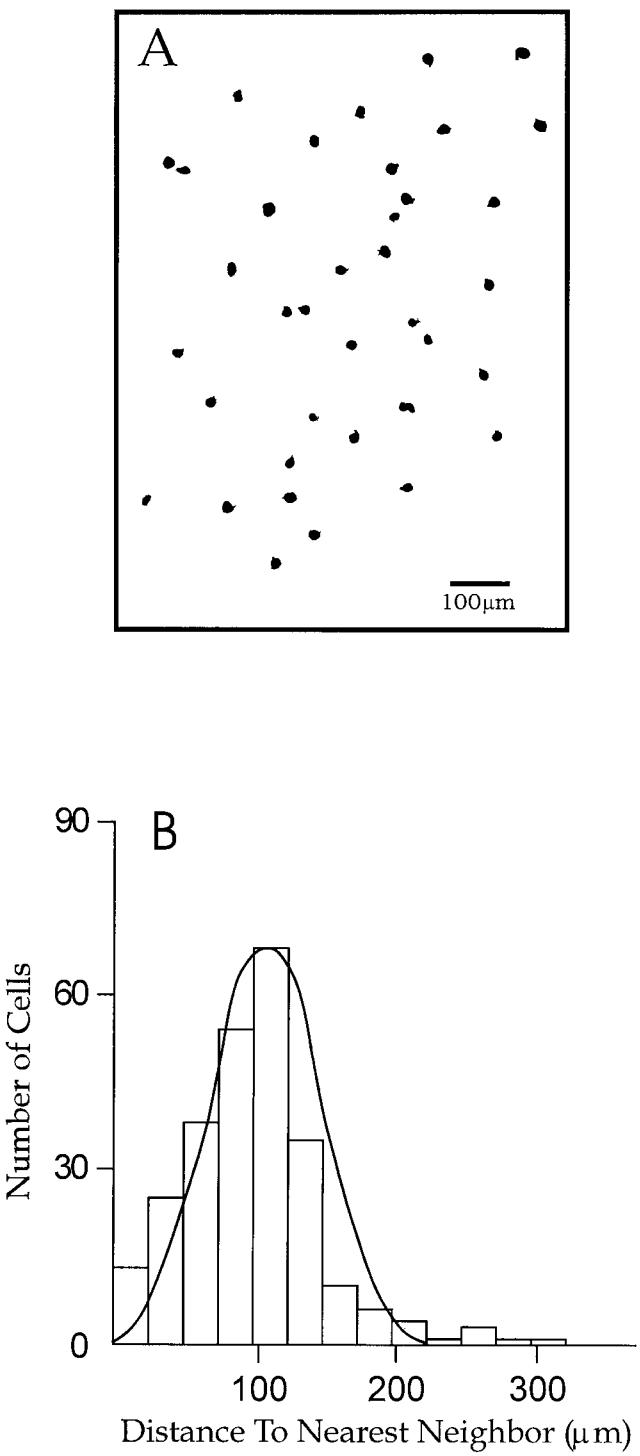

Fig. 13. **A:** Camera lucida tracing of CTB-positive ganglion cells from a randomly chosen region of gerbil whole-mount retina following CTB injection of the dorsal raphe nucleus. **B:** Frequency distribution (Gaussian) of nearest-neighbor intercellular distances (mean = 107 ± 4 μm).

be less critical in labeling retinal afferents. In CTB-labeled GCs of both species, conspicuous varicosities on primary and secondary dendrites resembled those described in other mammalian retinas (Peichl, 1989; Dann and Buhl, 1990; Pu and Amthor, 1990; Wingate et al., 1992; Zhan and Troy, 1997). However, the dendritic processes of many GCs appeared to be incompletely labeled with CTB; therefore, no reliable measures of dendritic field size, shape, or stratification patterns could be obtained. In gerbils, the estimated number of DRN-projecting GCs was 1,674, which is approximately 1% of the total GC population (Wickler et al., 1989).

Relationship of the DRN and visual system

In addition to its many ascending projections (Halliday, 1995), the DRN also innervates a number of retinorecipient nuclei, including the dorsal LGN, ventral LGN, IGL, SC, and visual cortex. DRN efferents to the dorsal LGN and SC originate from neurons located in the lateral cell groups (Villar et al., 1988; Waterhouse et al., 1993), the same region of the DRN that receives direct retinal input

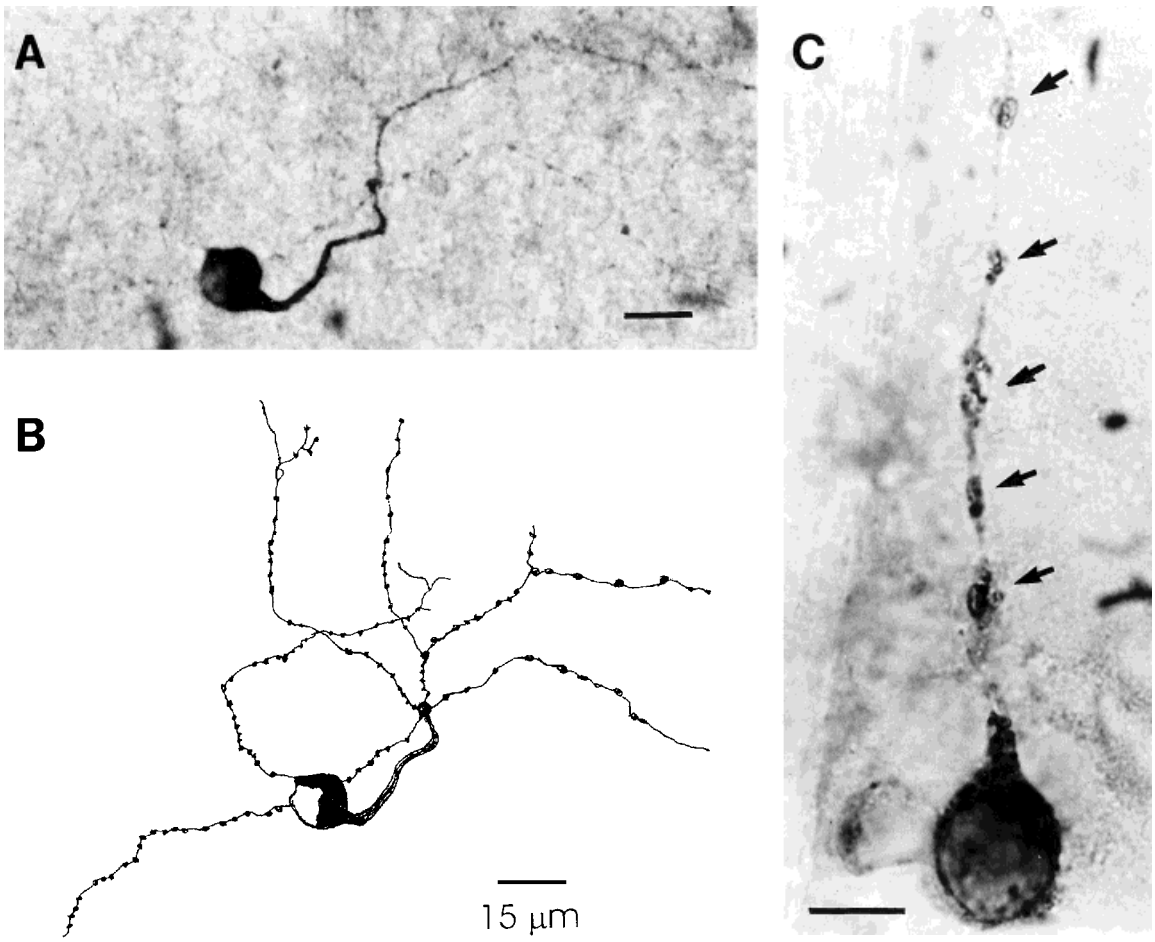

Fig. 14. **A:** CTB-positive ganglion cell in the rat retina following CTB injection into the dorsal raphe nucleus. **B:** Camera lucida tracing of ganglion cells shown in A. **C:** CTB-positive rat ganglion cell with conspicuous dendritic varicosities (arrows). Scale bars = 15 μm.

in both gerbils and rats; some DRN neurons reportedly project both to the LGN and to the SC (Villar et al., 1988). DRN neurons that project to rat visual cortex (areas 17, 18a, and 18b) have been described primarily in the ventromedial portion of the nucleus that lies between and dorsal to the medial longitudinal fasciculi (Waterhouse et al., 1993). Retinal afferents were observed in the ventromedial DRN in gerbils, but not in rats.

A dense, serotonergic projection to the superficial layers of the SC has been reported in mammals (Villar et al., 1988; Mize and Horner, 1989). Also, Mooney et al. (1996) investigated the distribution of 5-HT_{1A} and 5-HT_{1B} receptors in the SC and showed that 5-HT_{1B} receptors located on optic afferent terminals can exert presynaptic inhibition on retinocollicular input and that direct electrical stimulation of the lateral DRN reduced visually evoked responses of SC neurons. Other evidence indicates that activation of the DRN is associated with a pronounced inhibition of visual responsiveness in LGN neurons in rat and cat (Foote et al., 1974; Marks et al., 1987; Kayama et al., 1989; Xue et al., 1996). Although DRN neurons that project to central visual structures resemble the fusiform and multipolar neurons that contain serotonin (Descarries et al., 1982; Waterhouse et al., 1986, 1993), not all DRN efferent neurons are serotonergic (Villar et al., 1988; Koh et al., 1991).

Recently, in gerbils, a small population of neurons that project back to the retina was described in the ipsilateral DRN and adjacent PAG (Fite et al., 1997). These neurons also were observed in the present study; the majority had small somata and occurred within regions of the DRN that receive direct retinal afferents; however, they did not resemble DRN neurons that project to the LGN, SC, or visual cortex. Larsen and Moller (1985, 1987) also have described retinal efferents in gerbils, and other investigators have reported retinal efferent neurons in the DRN of rats (Itaya and Itaya, 1985; Villar et al., 1987), macaque monkeys, guinea pigs, and cats (Labandeira-Garcia et al., 1990). These DRN retinopetal neurons may constitute a centrifugal feedback loop such that effects of retinal input in the DRN may, in turn, influence retinal processing and/or retinal output.

The direct, retinal-DRN projection may be part of an increasingly well-documented system of retinal afferents that lie outside the boundaries of the classically defined central visual system. Pickard (1982, 1985) and Cooper et al. (1989, 1993) have proposed that this "nonimage-forming" component of mammalian central visual pathways mediates the photic regulation of the neuroendocrine and circadian systems via afferents that encode the temporal and photometric characteristics of environmental light rather than spatial information. A variety of anatomical,

histochemical, developmental, and electrophysiological characteristics appear to distinguish the nonimage-forming components of the mammalian visual system (Card and Moore, 1991; Ritter and Dinh, 1991; Martinet et al., 1992; Cooper et al., 1993; Mick et al., 1993; Enquist et al., 1994; Herbin et al., 1994) from those that mediate perceptual, oculomotor, and/or visuomotor functions.

One major component of this nonimage-forming system is the retinal-SCN and retinal-IGL-SCN circuitry associated with the neural control and modulation of circadian rhythms (Wetterberg, 1993; Morin, 1994; Takahashi, 1995; Moore, 1996; Harrington, 1997; Hastings, 1997). Electrophysiological response properties of retinohypothalamic afferents indicate that this pathway encodes information primarily about ambient illumination and photoperiodic variations (Meijer et al., 1986; Meijer and Rietveld, 1989; Morin, 1994). Direct retinal input to the SCN that is necessary for both circadian photic entrainment and phase shifts reportedly originates from a distinct population of retinal ganglion cells (Pickard, 1980; Moore et al., 1995). The SCN also receives second-order, optic input from neuropeptide Y (NPY)-containing neurons located in the IGL (Morin et al., 1992), and a subset of ganglion cells has been described that project both to the SCN and to the IGL (Pickard, 1985; Moore et al., 1995). A variety of experimental evidence now indicates that the IGL-SCN geniculohypothalamic tract mediates nonphotic entrainment of the circadian pacemaker (Morin, 1994; Moore and Card, 1994; Mrosovsky, 1996; Harrington, 1997; Maywood et al., 1997). In hamsters and rats, the DRN projects to the IGL and ventral LGN, and it has been suggested that circadian rhythms may be influenced, indirectly, via the DRN-IGL-SCN pathways (Meyer-Bernstein and Morin, 1996; Moga and Moore, 1997; Maywood et al., 1997). Also, electrical stimulation of the DRN has been shown to modulate circadian phase in hamsters (Rea et al., 1997), inducing an increase in 5-HT release and phase advances in circadian activity rhythms (Dinardo et al., 1998; Dudley et al., 1998; Meyer-Berstein and Morin, 1998).

From a somewhat broader perspective, relatively little is known about the ways in which environmental photic stimulation can influence arousal, affective, and/or emotional states via the serotonergic nuclei of the brainstem. Both experimental and clinical investigations of the nonperceptual aspects of visual stimulation have described the therapeutic effectiveness of light in regulating circadian rhythmicity and menstrual cyclicity and as an antidepressant in the treatment of seasonal affective disorder (Terman et al., 1990; Wetterberg, 1993; Terman, 1993; Oren and Terman, 1998). Considerable evidence now indicates that serotonergic mechanisms are involved in some seasonal types of depression (see Rosenthal and Blehar, 1989; Jacobsen et al., 1989; Lam et al., 1996, 1997). Other evidence indicates that light stimulation may directly effect serotonin levels in the DRN (Cagampang et al., 1993; Cagampang and Inouye, 1994) and other brain regions (Ferraro and Steger, 1990), except in the SCN, where an endogenous circadian rhythm in neuronal 5-HT release appears to occur in the absence of photic or environmental light cues (Dudley et al., 1998).

In conclusion, the direct, retinal-DRN projection described in the present report could be an important route by which environmental light may influence the activity and/or state of neurons in the DRN, with potential effects on a broad range of neural circuits and behaviors. From a comparative perspective, the more extensive retinal-DRN projection observed in gerbils may be associated with the more highly visual and crepuscular/diurnal habits of this species compared to rats, which are highly nocturnal. Whether comparable differences will be observed in other diurnal and noctural species remains to be determined. The functional significance of this unusual pathway is as yet unknown, in particular whether it is directly involved in neural circuits that underlie a variety of nonperceptual effects of light.

ACKNOWLEDGMENTS

We thank Ms. Janice Cosentino for her excellent histological assistance and Dr. Neil Berthier for valuable statistical advice.

LITERATURE CITED

Angelucci A, Clasca F, Sur M. 1996. Anterograde axonal tracing with the subunit of cholera toxin: a highly sensitive immunohistochemical protocol for revealing fine axonal morphology in adult and neonatal brains. J Neurosci Methods 5:101–112.

Cagampang FR, Inouye ST. 1994. Diurnal and circadian changes of serotonin in the suprachiasmatic nuclei: regulation by light and an endogenous pacemaker. Brain Res 639:175–179.

Cagampang FR, Yamazaki S, Otori Y, Inouye ST. 1993. Serotonin in the raphe nuclei: regulation by light and an endogenous pacemaker. Neuroreport 5:49–52.

Card JP, Moore RY. 1991. The organization of visual circuits influencing the circadian acitivity of the suprachiasmatic nucleus. In: Klein DC, Moore RY, Reppert SM, editors. Suprachiasmatic nucleus: the mind's clock. New York: Oxford University Press. p 51–76.

Cassel JC, Jeltsch H. 1995. Serotonergic modulation of cholinergic function in the central nervous: cognitive implications. Neuroscience 69:1–41.

Cook JE. 1996. Spatial properties of retinal mosaics: an empirical evaluation of some existing measures. Vis Neurosci 13:15–30.

Cook JE. 1998. Getting to grips with neuronal diversity: what is a neuronal type? In: Chalupa L, Finlay B, editors. Development and organization of the retina. New York: Plenum Press. p 91–120.

Cooper HM, Mick G, Magnin M. 1989. Retinal projection to mammalian telencephalon. Brain Res 477:350–357.

Cooper HM, Herbin M, Nevo E. 1993. Visual system of a naturally micropthalmic mammal: the blind mole rat, *Spalax ehrenbergi*. J Comp Neurol 328:313–350.

Dann JF, Buhl EH. 1990. Morphology of retinal ganglion cells in the flying fox (*Pteropus scapulatus*): a Lucifer yellow investigation. J Comp Neurol 301:401–416.

Descarries L, Watkins KC, Garcia S, Beaudet A. 1982. The serotonin neurons in nucleus raphe dorsalis of adult rat: a light and electron microscope radioautographic study. J Comp Neurol 207:239–254.

Dinan TG. 1996. Serotonin and the regulation of hypothalamic-pituitary-adrenal axis function. Life Sci 58:1683–1694.

Dinardo LA, Dudley E, Glass JD. 1998. Pharmacological and electrical manipulations of median and dorsal raphe activity: effects on 5-HT release in hamster SCN. Soc Res Biol Rhythms 6:79.

Dudley TE, DiNardo LA Jr, Ehlen C, Glass JD. 1998. Further evidence for a role of the dorsal raphe in hamster circadian regulation. Soc Res Biol Rhythms 6:79.

Enquist LW, Dubin J, Whealy ME, Card JP. 1994. Complementation analysis of pseudorabies virus gE and gI mutants in retinal ganglion cells neurotropism. J Virol 68:5275–5279.

Ferraro JS, Steger RW. 1990. Diurnal variations in brain serotonin are driven by the photic cycle and are not circadian in nature. Brain Res 512:121–124.

Fite KV, Janusonis S, Foote W, Bengston L, Cosentino J. 1997. Retinofugal and retinopetal pathways in the dorsal raphe and periaqueductal gray of the Mongolian gerbil. Soc Neurosci Abstr 23:1819.

Foote WE, Maciewicz RJ, Mordes JP. 1974. The effect of midbrain raphe and lateral mesencephalic stimulation on spontaneous and evoked activity in the lateral geniculate of the cat. Exp Brain Res 19:124–130.

Foote WE, Taber-Pierce E, Edwards L. 1978. Evidence for retinal projection to the midbrain raphe of the cat. Brain Res l56:135–140.

Govardovskii VI, Rohlich P, Szel A, Khokhlova TV. 1992. Cones in the retina of the Mongolian gerbil, *Meriones unguiculatus*: an immunocytochemical and electrophysiological study. Vis Res 32:19–27.

Halliday G, Harding A, Paxinos G. 1995. Serotonin and tachykinin systems. In: Paxinos G, editor. The rat nervous system, 2nd ed. New York: Academic Press. p 929–973.

Harrington ME. 1997. The ventral lateral geniculate nuclues and the intergeniculate leaflet: interrelated structures in the visual and circadian systems. Neurosci Biobehav Rev 21:705–727.

Harvey JA. 1996. Serotonergic regulation of associative learning. Behav Brain Res 73:47–50.

Hastings MH. 1997. Central clocking. Trends Neurosci 20:459–463.

Herbin M, Reperant J, Cooper HM. 1994. Visual system of the fossorial mole-lemings, *Ellobius talpinus* and *Ellobius lutescens*. J Comp Neurol 346:253–275.

Huxlin KR, Goodchild AK. 1997. Retinal ganglion cells in the albino rat: revised morphological classification. J Comp Neurol 385:309–323.

Itaya SK, Itaya PW. 1985. Centrifugal fibers to the rat retina from the medial pretectal area and the periaqueductal grey matter. Brain Res 326:362–365.

Jacobs BL, Fornal CA. 1993. 5-HT and motor control: a hypothesis. Trends Neurosci 16:346–352.

Jacobson FM, Murphy DL, Rosenthal NE. 1989. The role of serotonin in seasonal affective disorder and the antidepressant response to phototherapy. In: Rosenthal NE, Blehar MC, editors. Seasonal affective disorders and phototherapy. New York: The Guilford Press. p 333–341.

Kawano H, Decker K, Reuss S. 1996. In there a direct retina-raphe-suprachiasmatic pathway in the rat? Neurosci Lett 212:143–146.

Kayama Y, Shimada S, Hishikawa Y, Ogawa T. 1989. Effects of stimulating the dorsal raphe nucleus of the rat on neuronal activity in the dorsal lateral geniculate nucleus. Brain Res 489:1–11.

Koh T, Nakazawa M, Kani K, Maeda T. 1991. Significant non-serotonergic raphe projections to the visual cortex of the rat. An immunohistochemical study combined with retrograde tracing. J Hirnforsch 6:707–714.

Labandeira-Garcia JL, Guerra-Seijas MJ, Gonzalez F, Perez R, Acuna C. 1990. Location of neurons projecting to the retina in mammals. Neurosci Res 8:291–302.

Lam RW, Zis AP, Grewal A, Delgado PL, Charney DS, Krystral JH. 1996. Effects of rapid tryptophan depletion in patients with seasonal affective disorder in remission after light therapy. Arch Gen Psychiatr 53:41–44.

Lam RW, Terman M, Wirz-Justice A. 1997. Light therapy for depressive disorders: indications and efficacy. In: Rush AJ, editor. Mood disorders. Systematic medication management. Mod Probl Pharmacopsychiatr 25:215–234.

Larsen JNB, Moller M. 1985. Evidence for efferent projections from the brain to the retina of the Mongolian gerbil (*Meriones unguiculatus*). A horseradish peroxidase tracing study. Acta Ophthalmol 63:11–14.

Larsen JNB, Moller M. 1987. The presence of retinopetal fibres in the optic nerve of the Mongolian gerbil (*Meriones unguiculatus*): a horseradish peroxidase in vitro study. Exp Eye Res 45:763–768.

Leak RK, Moore RY. 1997. Identification of retinal ganglion cells projecting to the lateral hypothalamic area of the rat. Brain Res 770:105–114.

Ling C, Schneider GE, Jhaveri S. 1998. Target-specific morphology of retinal axon arbors in the adult hamster. Vis Neurosci 15:559–579.

Marks GA, Speciale SG, Cobbey K, Roffwarg HP. 1987. Serotonergic inhibition of the dorsal lateral geniculate nucleus. Brain Res 418:76–84.

Martinet L, Serviere J, Peytevin J. 1992. Direct retinal projections of the "non-image forming" system to the hypothalamus, anterodorsal thalamus and basal telencephalon of mink (*Mustela vison*) brain. Exp Brain Res 89:373–382.

Maywood ES, Smith E, Hall SJ, Hastings MH. 1997. A thalamic contribution to arousal-induced, non-photic entrainment of the circadian clock of the Syrian hamster. Eur J Neurosci 9:1739–1747.

Medanic M, Gillette MU. 1992. Serotonin regulates the phase of the rat suprachiasmatic circadian pacemaker in vitro only during the subjective day. J Physiol (London) 450:629–642.

Meijer JH, Rietveld WJ. 1989. Neurophysiology of the suprachiasmatic circadian pacemaker in rodents. Physiol Rev 69:671–707.

Meijer JH, Groos GA, Rusak B. 1986. Luminance coding in a circadian pacemeaker: the suprachiasmatic nucleus of the rat and hamster. Brain Res 382:109–118.

Meyer-Bernstein EL, Morin LP. 1996. Differential serotonergic innervation of the suprachiasmatic nucleus and the intergeniculate leaflet and its role in circadian rhythm modulation. J Neurosci 16:2097–2111.

Meyer-Bernstein EL, Morin LP. 1998. Electrical stimulation of the median (MR) or dorsal raphe (DR) nuclei elicits circadian rhythm phase shifts in the hamster. Soc Neurosci Abstr 24:1918.

Meyer-Bernstein EL, Blanchard JH, Morin LP. 1997. The serotonergic projection from the median raphe nucleus to the suprachiasmatic nucleus modulates activity phase onset, but not other circadian rhythm parameters. Brain Res 755:112–120.

Mick G, Cooper H, Magnin M. 1993. Retinal projection to the olfactory tubercle and basal telencephalon in primates. J Comp Neurol 327:205–219.

Mikkelsen JD. 1992. Visualization of efferent retinal projections by immunohistochemical identification of cholera toxin subunit B. Brain Res Bull 28:619–623.

Mitrofanis J, Finlay BL. 1990. Developmental changes in the distribution of retinal catecholaminergic neurons in hamsters and gerbils. J Comp Neurol 292:480–494.

Mize RR, Horner LH. 1989. Origin, distribution, and morphology of serotonergic afferents to the cat superior colliculus: a light and electron microscope immunocytochemistry study. Exp Brain Res 75:83–98.

Moga M, Moore RY. 1997. The organization of neural inputs to the suprachiasmatic nucleus in the rat. J Comp Neurol 389:508–534.

Montgomery S. 1995. Serotonin, sertraline and depression. J Psychopharmacol 9:179–184.

Mooney RD, Huang X, Shi MY, Bennett-Clarke CA, Rhoades RW. 1996. Serotonin modulates retinotectal and corticotectal convergence in the superior colliculus. Progr Brain Res 112:57–69.

Moore RY. 1996. Neural control of the pineal gland. Behav Brain Res 73:125–130.

Moore RY, Card PY. 1994. Intergeniculate leaflet: an anatomically and functionally distinct subdivision of the lateral geniculate complex. J Comp Neurol 344:403–430.

Moore RY, Speh JC, Card JP. 1995. The retinohypothalamic tract originates from a distinct subset of retinal ganglion cells. J Comp Neurol 352:351–366.

Morin LP. 1994. The circadian visual system. Brain Res Rev 67:102–127.

Morin LP, Blanchard JH, Moore RY. 1992. Intergeniculate leaflet and suprachiasmatic nuclear organization and connections in the hamster. Vis Neurosci 8:219–230.

Mrosovsky N. 1996. Locomotor activity and non-photic influences on circadian clocks. Biol Rev 71:343–372.

Oren DA, Terman M. 1998. Tweaking the human circadian clock with light. Science 279:333–334.

Paxinos G, Watson C. 1998. The rat brain in stereotaxic coordinates, 4th ed. Sydney: Academic Press.

Peichl L. 1989. Alpha and delta ganglion cells in the rat retina. J Comp Neurol 286:120–139.

Pickard GE. 1980. Morphological characteristics of retinal ganglion cells projecting to the suprachiasmatic nucleus: a horseradiash peroxidase study. Brain Res 183:458–465.

Pickard GE. 1982. The afferent connections of the suprachiasmatic nucleus of the golden hamster with emphasis on the retinohypothalamic projection. J Comp Neurol 211:65–83.

Pickard GE. 1985. Bifurcating axons of retinal ganglion cells terminate in the hypothalamic suprachiasmatic nucleus and the intergeniculate leaflet of the thalamus. Neurosci Lett 55:211–217.

Portas CM, Bjorvatn B, Fagerland S, Gronli J, Mundal V, Sorensen E, Ursin R. 1998. On-line detection of extracellular levels of serotonin in dorsal raphe nucleus and frontal cortex over the sleep/wake cycle in the freely moving rat. Neuroscience 83:807–814.

Prosser RA, Dean RR, Edgar DM, Heller HC, Miller JD. 1993. Serotonin and the mammalian circadian system. I. In vitro phase shifts by serotonergic agonists and antagonists. J Biol Rhythms 8:1–16.

Pu ML, Amthor FR. 1990. Dendritic morphologies of retinal ganglion cells projecting to the lateral geniculate nucleus in the rabbit. J Comp Neurol 302:675–693.

Qu T, Dong D, Sugioka K, Yamadori T. 1996. Demonstration of direct input from the retina to the lateral habenular nucleus in the albino rat. Brain Res 779:251–258.

Rea MA, Cato MJ, Weber ET. 1997. Electrical stimulation of the dorsal raphe nucleus modulates circadian phase in hamsters. Soc Neurosci Abstr 23:790.

Ritter S, Dinh TT. 1991. Prior optic nerve transection reduces capsaicin-induced degeneration in the rat subcortical visual structures. J Comp Neurol 308:79–90.

Rosenthal NE, Blehar MC. 1989. Seasonal affective disorders and phototherapy. New York: The Guilford Press.

Shen H, Semba K. 1994. A direct retinal projection to the dorsal raphe nucleus in the rat. Brain Res 635:159–168.

Simansky KJ. 1996. Serotonergic control of the organization of feeding and satiety. Behav Brain Res 73:37–42.

Stamp JA, Semba K. 1995. Extent of colocalization of serotonin and GABA in the neurons of the rat raphe nuclei. Brain Res 677:39–49.

Susic V, Masirevic G. 1986. Sleep patterns in the Mongolian gerbil, *Meriones unguiculatus*. Physiol Behav 37:257–261.

Takahashi JS. 1995. Molecular neurobiology and genetics of circadian rhythms in mammals. Annu Rev Neurosci 18:531–553.

Terman M. 1993. Light treatment. In: Kruger M, Roth T, Dement W, editors. Principles and practice of sleep medicine. Philadelphia: W.B. Saunders. p 1012–1029.

Terman M, Reme CE, Rafferty B, Gallin PF, Terman JS. 1990. Bright light therapy for winter depression: potential ocular effects and theoretical implications. Photochem Photobiol 51:781–792.

Vertes RP. 1991. A PHA-L analysis of ascending projections of the dorsal raphe nucleus in the rat. J Comp Neurol 313:643–668.

Villar MJ, Vitale ML, Parisi MN. 1987. Dorsal raphe serotonergic projection to the retina. A combined peroxidase tracing-neurochemical/high-performance liquid chromatography study in the rat. Neuroscience 22:681–686.

Villar MJ, Vitale MH, Hokfelt T, Verhofstad AAJ. 1988. Dorsal raphe serotoninergic branching neurons projecting both to the larteral geniculate body and superior colliculus: a combined retrograde tracing-immunohistochemical study int he rat. J Comp Neurol 277:126–140.

Waterhouse BD, Mihaloff GA, Baack JC, Woodward DJ. 1986. Topographical distribution of dorsal and median raphe neurons projecting to motor, sensorimotor and visual cortical areas in the rat. J Comp Neurol 249:460–476.

Waterhouse BD, Border B, Wahl L, Mihailoff GA. 1993. Topographic organization of rat locus coeruleus and dorsal raphe nuclei: distribution of cells projecting to visual system structures. J Comp Neurol 336:345–361.

Wetterberg L, editor. 1993. Light and biological rhythms in man. New York: Pergamon Press.

Wickler KC, Perez G, Finlay BL. 1989. Duration of retinogenesis: its relationship to retinal organization in two cricetine rodents. J Comp Neurol 285:157–176.

Wiklund L, Leger L, Persson M. 1981. Monoamine cell distribution in the cat brain. A fluorescence histochemical study with quantification of indolaminergic and locus coeruleus cell groups. J Comp Neurol 203:613–647.

Wingate RJ, Fitzgibbon T, Thompson ID. 1992. Lucifer yellow, retrograde tracers, and fractal analysis characterise adult ferret ganglion cells. J Comp Neurol 323:449–474.

Xue JT, Harting JK, Uhlrich DJ. 1996. Dorsal raphe and tuberomammillary nuclei modulate visual responses and firing mode of LGN relay cells. Soc Neurosci Abstr 22:1606.

Youngstrom TG, Weiss ML, Nunez AA. 1991. Retinofugal projections to the hypothalamus, anterior thalamus and basal forebrain in hamsters. Brain Res Bull 26:403–411.

Zhan XJ, Troy JB. 1997. An efficient method that reveals both dendrites and the soma mosiacs of retinal ganglion cells. J Neurosci Methods 72:109–116.